

# Signature of Wave Chaos in Spectral Characteristics of Microcavity Lasers

Satoshi Sunada<sup>1</sup>, Susumu Shinohara<sup>2</sup>, Takehiro Fukushima<sup>3</sup>, and Takahisa Harayama<sup>4</sup>

<sup>1</sup>*Faculty of Mechanical Engineering, Institute of Science and Engineering,  
Kanazawa University, Kakuma-machi Kanazawa, Ishikawa 920-1192, Japan*

<sup>2</sup>*NTT Communication Science Laboratories, NTT Corporation,  
2-4 Hikaridai Seika-cho Soraku-gun, Kyoto 619-0237, Japan*

<sup>3</sup>*Department of Information and Communication Engineering,  
Okayama Prefectural University, 111 Kuboki Soja, Okayama 719-1197, Japan*

<sup>4</sup>*Department of Applied Physics, School of Advanced Science and Engineering,  
Waseda University, 3-4-1 Okubo, Shinjuku-ku, Tokyo 169-8555, Japan*

(Dated: May 28, 2019)

We report the spectral characteristics of fully chaotic and non-chaotic microcavity lasers under continuous-wave operating conditions. It is found that fully chaotic microcavity lasers operate in single mode, whereas non-chaotic microcavity lasers operate in multimode. The suppression of multimode lasing for fully chaotic microcavity lasers is explained by large spatial overlaps of the resonance wave functions that spread throughout the two-dimensional cavity due to the ergodicity of chaotic ray orbits.

PACS numbers: 42.55.Sa, 05.45.Mt, 42.55.Px

Various active devices ranging from musical instruments to lasers generate oscillating states with well-defined frequencies from the interplay between resonator geometry and an active nonlinear element [1–3]. Understanding and controlling the formations of such self-organized oscillating states is important in device physics and related applications. As a specific example, two-dimensional (2D) microcavity lasers have attracted considerable attention because they can offer a new platform for experimentally addressing fundamental issues such as quantum/wave chaos in open systems [4–6] and non-Hermitian physics [7, 8]. The studies of 2D microcavity lasers have also led to a wide range of applications, including low-threshold microlasers with unidirectional emission [9–13], low-coherence microlasers [14], and fast random signal generation [15].

An important characteristic of 2D microcavity lasers is the emission pattern. It has been shown that the emission patterns can be well explained by resonance modes (i.e., the eigenmodes in passive cavities), even when the cavity is chaotic, i.e., the ray dynamics within the cavity are chaotic [3–5]. Up to now, significant effort has been devoted to understanding and designing passive resonance characteristics [16–22].

However, the lasing spectrum, another important lasing characteristic, cannot be fully explained by the passive resonance characteristics alone. This is mainly due to modal interactions induced by nonlinearity (i.e., saturation) of the laser gain medium. A gain competition induces complex but interesting interactions among modes: when one mode is excited, the mode suppresses the lasing of the other modes. Without considering such interactions, one cannot precisely predict how many modes can be excited. Understanding gain competition is an important subject in laser physics, although conventionally, one-dimensional cavities are mainly studied [23–25]. Unlike one-dimensional cavities, 2D cavities typically have

modes with complex spatial patterns, and the openness of the cavities greatly influences the modal patterns. In previous works, chaotic microcavity lasers have been numerically studied from the viewpoint of modal interactions and have been shown to exhibit a rich variety of nonlinear phenomena [26–30]. Steady lasing states fully incorporating the nonlinearity and openness of the cavities are being intensively studied [14, 31, 32]. Fundamental questions are how modal interaction influences the lasing characteristics of 2D microcavities having complex modes and what differences arise according to the cavity shapes. The purpose of this paper is to address these questions by systematically investigating the spectra of 2D semiconductor microcavity lasers under continuous-wave (cw) operating conditions. In this work, we focus on two types of laser cavities, fully chaotic and non-chaotic cavities where almost all ray orbits in the former are chaotic and none of the ray orbits in the latter are chaotic. We identify a striking difference in their lasing spectra. We show that fully chaotic cavity lasers exhibit strong suppression of multimode lasing and operate in single mode regardless of the size and deformation parameters, whereas non-chaotic cavity lasers operate in multimode. This difference is explained by the intrinsic difference in modal patterns between fully chaotic and non-chaotic cavities.

In this work, we focus on a specific shape of the fully chaotic cavity called the stadium, defined in Fig. 1(a). Its full chaoticity has been rigorously proven [33]. The stadium cavity consists of two straight lines of length  $l$  and two half circles of radius  $R$ . We define the aspect ratio parameter  $p = W/L$ , where  $W = 2R$  is the length of the minor axis and  $L = 2R + l$  is the length of the major axis. For the non-chaotic cavity, we focus on the elliptic cavity defined in Fig. 1(b). It is known that a closed elliptic cavity is an integrable system [34], thus exhibiting no chaotic behavior. In the same manner as for

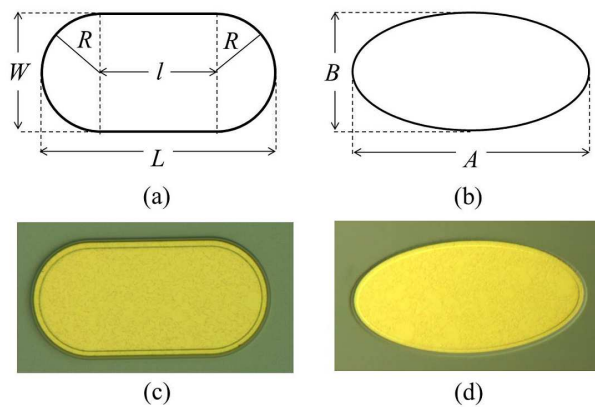


FIG. 1: (Color online) (a) Stadium cavity and (b) elliptic cavity. (c)(d) Optical microscope images of the fabricated lasers, where both cavities have an area  $S = 8748 \mu\text{m}^2$  and an aspect ratio  $p = 0.5$ .

the stadium cavity, we define the aspect ratio parameter for the elliptic cavity as  $p = B/A$ , where  $A$  and  $B$  are the lengths of the major and minor axes, respectively.

We fabricated semiconductor microcavities with the stadium and elliptic cavities by applying a reactive-ion-etching technique to a graded index separate-confinement-heterostructure (GRIN-SCH) single-quantum-well GaAs/Al<sub>x</sub>Ga<sub>1-x</sub>As structure grown by MOCVD (See [35] for details on the layer structures and fabrication process). The fabricated lasers are shown in Figs. 1(c) and 1(d). In our experiments, the lasers were soldered onto aluminum nitride submounts at  $20 \pm 0.1$  °C and electrically driven with cw current injection. The optical outputs were collected with anti-reflection-coated lenses and coupled to a multimode optical fiber via a 30-dB optical isolator.

Figure 2 shows the lasing spectra for the stadium cavity laser with cavity area  $S = 8748 \mu\text{m}^2$  and  $p = 0.5$  ( $R = 35 \mu\text{m}$  and  $l = 70 \mu\text{m}$ ). Because of the large area, the number of modes within the gain band was estimated to be a few thousand. Nevertheless, interestingly, the lasing spectra exhibit only a single sharp peak regardless of the current value  $I$ . The peak is continuously red-shifted due to a thermal effect as  $I$  increases. As shown in the inset of Fig. 2, the linewidth of the peak is approximately 0.004 nm, which is close to the resolution limit of 0.002 nm of our spectrum analyzer (Advantest Q8347). For further evidence on single-mode lasing (i.e., single-wavelength lasing), we measured the power spectrum of the output intensity using a photodetector with a bandwidth of 12.5 GHz and confirmed that there were no beat frequencies due to multimode lasing in the spectrum [30]. In addition, we evaluated the number of lasing modes by measuring the contrast of the far-field emission pattern [36]. Using a relationship between the contrast and the number of lasing modes [14], we obtained a result that suggests single-mode operation.

Figure 3 shows the lasing spectra for the elliptic cavity

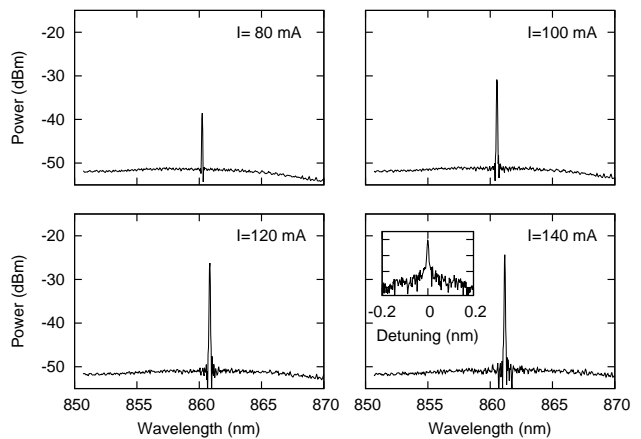


FIG. 2: Spectra of the stadium cavity laser with a cavity area  $S = 8748 \mu\text{m}^2$  and an aspect ratio  $p = 0.5$  for various current values. The threshold current is approximately 74 mA.

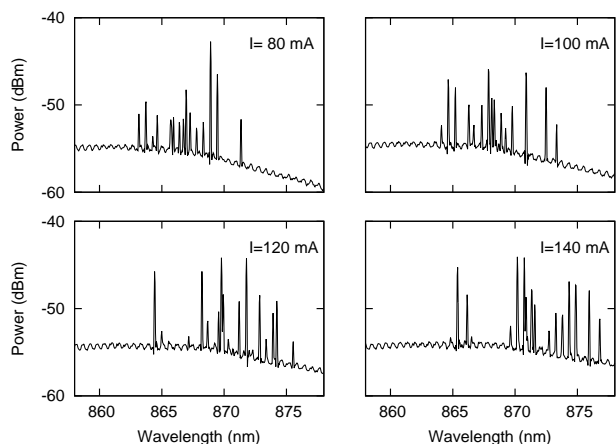


FIG. 3: Spectra of the elliptic cavity laser with a cavity area  $S = 8748 \mu\text{m}^2$  and an aspect ratio  $p = 0.5$  for various current values. The threshold current is approximately 34 mA.

laser with the same area and aspect ratio as the above stadium cavity laser. As compared to Fig. 2, there is a remarkable difference in the appearance of multiple peaks. In order to quantify the difference of the spectral characteristics between the two lasers, we counted the number of lasing peaks whose intensities were larger than  $-20$  dB of the maximum peak in each spectrum. Figure 4 shows the number of peaks as a function of the current normalized by the threshold value  $I_{th}$  for each laser. As shown in Fig. 4, the difference in the number of peaks between the two lasers increases as  $I$  increases. We also investigated the spectral characteristics for various cavity areas with a fixed  $p$ -value and found similar tendencies toward a single-mode lasing state for the stadium cavity lasers and toward a multimode lasing state for elliptic cavity lasers. As a slight exception, we observed two peaks for the stadium cavity laser for the normalized current  $I/I_{th}$

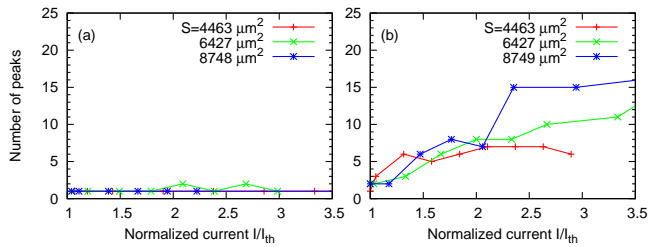


FIG. 4: (Color online) Injection current dependence of the number of peaks in the spectra of (a) the stadium cavity lasers and (b) the elliptic cavity lasers with various cavity areas  $S$ . In both (a) and (b), the aspect ratio is  $p = 0.5$ .

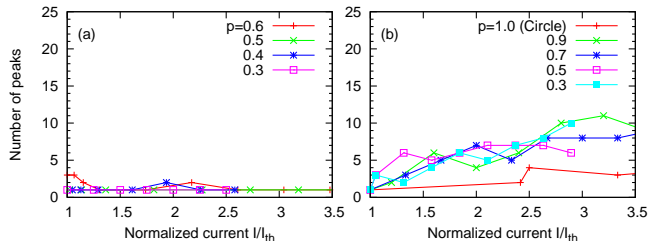


FIG. 5: (Color online) Injection current dependence of the number of peaks in the spectra of (a) the stadium cavity lasers and (b) the elliptic cavity lasers with various aspect ratios  $p$ . In (a), the radius  $R$  is fixed as  $25 \mu\text{m}$ , (i.e., the area for  $p = 0.5$  is  $S = 4463 \mu\text{m}^2$ ). In (b), the areas of the elliptic cavities are the same as that of the stadium cavity with  $p = 0.5$ .

= 2.1 and 2.7 in Fig. 4(a). We attribute this to mode hopping caused by a thermal effect of the current injection, such as a gain shift and change in the refractive index.

Even with changing the aspect ratios of the cavities, we found similar spectral characteristics. Figure 5(a) shows the current dependence of the number of peaks for the stadium cavity lasers with various  $p$ -values, where the radius  $R$  is fixed as  $25 \mu\text{m}$ . The results for elliptic cavity lasers with various  $p$ -values are shown in Fig. 5(b).  $p = 1$  corresponds to the circular cavity, which is categorized as a non-chaotic cavity. There is a possibility that the number of peaks has been underestimated because some modes have such weak outputs (due to high confinement) that they cannot be captured in the far field. With the deformation toward the stadium shape (i.e.,  $p < 1$ ), the number of peaks decreases and single-mode lasing can be achieved for high current values [Fig. 5(a)]. On the other hand, the deformation toward the ellipse does not exhibit the transition to single-mode lasing; the multimode lasing state is maintained [Fig. 5(b)].

As these experiments indicate, strong suppression of multimode lasing is a common feature of stadium cavity lasers. As discussed in [23–25], a competitive interaction occurs among modes that are overlapped not only spectrally but also spatially. In a fully chaotic cavity, modes

typically have complex spatial patterns spread throughout the entire cavity [for a typical example, see Fig. 6(a)], resulting in large spatial overlaps with other modes. Actually, previous numerical simulations of stadium cavity lasers demonstrated strong selection of lasing modes owing to a competitive interaction [27, 28, 30]. Moreover, a frequency-locking phenomenon occurs among several lasing modes, which integrates them into a single lasing mode [27, 29, 30]. On the other hand, non-chaotic cavities typically support spatially localized modes, e.g., whispering-gallery modes in circular and elliptic cavities. When modes are spatially localized around different areas, as shown in Figs. 6(c) and 6(d), and the spatial overlap is small, the competition can be avoided between them. Indeed, simultaneous lasing of multiple whispering-gallery modes for a circular cavity laser was numerically demonstrated in Ref. [37].

The above discussion suggests that spatial modal overlapping is a necessary condition of the modal interaction that suppresses simultaneous lasing. To quantify the spatial overlaps between two modes, we introduce the following cross-correlation for the amplitude distributions of resonance modes:

$$C = \frac{\int |\phi(\mathbf{r})| |\psi(\mathbf{r})| w(\mathbf{r}) d\mathbf{r}}{\sqrt{\left( \int |\phi(\mathbf{r})|^2 w(\mathbf{r}) d\mathbf{r} \right) \left( \int |\psi(\mathbf{r})|^2 w(\mathbf{r}) d\mathbf{r} \right)}}, \quad (1)$$

where  $\phi(\mathbf{r})$  and  $\psi(\mathbf{r})$  are the modal wave functions and  $w(\mathbf{r})$  represents a pumping region. For uniform pumping,  $w(\mathbf{r}) = 1$  inside the cavity, whereas  $w(\mathbf{r}) = 0$  outside. The correlation is essentially similar to a spatial contribution to the cross-gain saturation (i.e., intensity cross-correlation) between two modes [23–25, 38]. By using the boundary element method [39], we calculated the resonances of the stadium and elliptic cavities with  $p = 0.5$ , imposing a refractive index of 3.3 inside the cavities and transverse electric (TE) polarization. Because of computational power limitations, we set the size parameter  $2\pi R/\lambda \approx 100$ , where  $R$  and  $\lambda$  are the characteristic radius and wavelength, respectively. This size parameter value is smaller than the real cavity sizes used in the experiments but large enough to discuss the properties of wave functions in the short-wavelength regimes [40]. We obtained approximately 100 low-loss modes with a quality factor  $Q \geq 3000$  for the stadium cavity, whereas  $Q \geq 3 \times 10^5$  for the elliptic cavity. Figure 7 shows the histogram of the spatial overlap  $C$  between two low-loss modes for the two cavities. The  $C$ -values for the stadium cavity are distributed around 0.77. It is known that several low-loss modes in chaotic cavities are so-called scarred modes [41, 42] whose intensities are localized along unstable periodic ray orbits [e.g., see Fig. 6(b)]. An interesting finding is that there is a large overlap ( $C \approx 0.73$ ) even for scarred modes. This is explained by the fact that the localization of the scarred modes is generally weak and significant intensities are spread throughout the cavity.

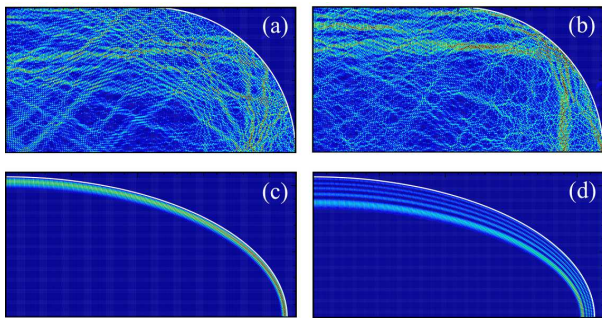


FIG. 6: (Color online) (a)(b) Spatial intensity patterns of low-loss modes for the stadium cavity, where (b) is a scarred mode with localization along a rectangular ray orbit. (c)(d) Spatial intensity patterns of whispering-gallery modes for the elliptic cavity, where the radial mode number is  $n_r = 1$  for (c) and  $n_r = 5$  for (d).

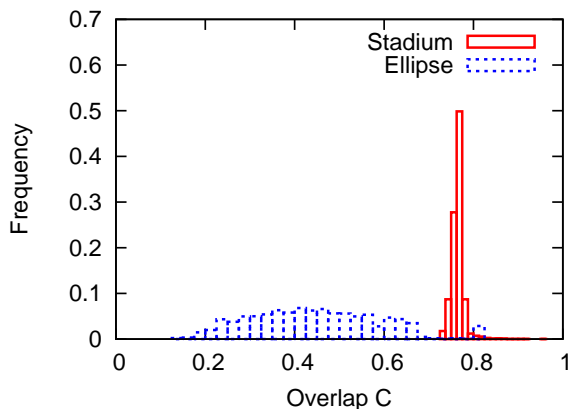


FIG. 7: (Color online) Histogram of overlap  $C$  defined by Eq. (1) between two low-loss modes for the stadium cavity (solid) and elliptic cavity (dotted).

In contrast, the  $C$ -values for the elliptic cavity are widely distributed with the mean value 0.45. The relatively low  $C$ -values come from the small spatial overlaps between the localized modes. In particular, the overlaps are small between two modes with different radial mode numbers  $n_r$ , which characterize the number of field max-

ima in the radial direction. For instance, the  $C$ -value between the modes with  $n_r = 1$  [Fig. 6(c)] and with  $n_r = 5$  [Fig. 6(d)] is only 0.14. As seen in Fig. 3, the lasing peaks in the spectra of the elliptic cavity laser are not always equally spaced. This result means that modes with different  $n_r$ -values were involved in the lasing, which supports our interpretation of the relation between the spatial overlaps and the spectral characteristics.

Lastly, we emphasize that the difference in the spectral characteristics between the stadium and elliptic cavity lasers was observed under the cw operating condition. Under the cw operating condition, single-mode lasing has been also reported for the other chaotic cavities with different shapes and different gain materials [43, 44]. However, under pulsed operating conditions, multimode emission can be observed even for fully chaotic cavity lasers [14, 40–42, 45, 46]. For example, in Ref. [30], multimode lasing has been observed in a stadium cavity laser for a pumping pulse width of  $\lesssim 100 \mu\text{s}$  (see Fig. 11 of Ref. [30] for details). The result can be partially attributed to transient slow mode-dynamics towards a steady lasing state [30].

In summary, we experimentally investigated and found a significant difference between the spectral characteristics of fully chaotic cavity lasers with a stadium shape and non-chaotic cavity lasers with an elliptic shape under the cw operating condition. In the stadium cavity lasers, regardless of the size and aspect ratio, only a single mode was excited at high pumping regimes, whereas many modes were excited in the elliptic cavity lasers. The strong suppression of multimode lasing observed in the stadium cavity lasers can be explained by large spatial overlaps between the low-loss modes. Because it is a common feature of fully-chaotic cavities that the modal pattern spreads throughout the cavity, we expect that the modal suppression leading to single-mode lasing is a universal feature of fully chaotic cavity lasers.

The authors would like to gratefully acknowledge Professor A. D. Stone and Professor H. Cao for fruitful discussions and insightful comments. This work was partially supported by Grant-in-Aid for Young Scientists (B) (Grant No. 26790056) from the MEXT of Japan.

- 
- [1] T. Idogawa, T. Kobata, K. Komuro, and M. Iwaki, *J. Acoust. Soc. Am.* **93**, 540 (1993); M. E. McIntyre, R. T. Schumacher, and J. Woodhouse, *J. Acoust. Soc. Am.* **74**, 1325 (1983).
- [2] H. Haken, *Synergetics. An Introduction, Nonequilibrium Phase Transitions and Self-organization in Physics, Chemistry, and Biology*, (Springer, Berlin, 1977).
- [3] T. Harayama and S. Shinohara, *Laser Photonics Rev.* **5**, 247 (2011).
- [4] J. U. Nöckel and A. D. Stone, *Nature* **385**, 45 (1997).
- [5] C. Gmachl, F. Cappasso, E. E. Narimanov, J. U. Nöckel, A. D. Stone, J. Faist, D. L. Sivco, and A. Y. Cho, *Science* **280**, 1556 (1998).
- [6] H. Cao and J. Wiersig, *Rev. Mod. Phys.* **87**, 61 (2015).
- [7] M. Liertzer, L. Ge, A. Cerjan, A. D. Stone, H. E. Türeci, and S. Rotter, *Phys. Rev. Lett.* **108**, 173901 (2012); M. Brandstetter, M. Liertzer, C. Deutsch, P. Klang, J. Schöberl, H. E. Türeci, G. Strasser, K. Unterrainer, and S. Rotter, *Nat. Commun.* **5**, 4034 (2014).
- [8] B. Peng, S. K. Özdemir, S. Rotter, H. Yilmaz, M. Liertzer, F. Monifi, C. M. Bender, F. Nori, L. Yang, *Science* **346**, 328 (2014).
- [9] J. Wiersig, M. Hentschel, *Phys. Rev. Lett.* **100**, 033901 (2008).

- [10] C. Yan, Q. J. Wang, L. Diehl, M. Hentschel, J. Wiersig, N. Yu, C. Pflügl, F. Capasso, M. A. Belkin, T. Edamura, M. Yamanishi, and H. Kan, *Appl. Phys. Lett.* **94**, 251101 (2009).
- [11] Q. Song, W. Fang, B. Liu, S.-T. Ho, G. S. Solomon, and H. Cao, *Phys. Rev. A* **80**, 041807(R) (2009).
- [12] C.-H. Yi, M.-W. Kim, and C.-M. Kim, *Appl. Phys. Lett.* **95**, 141107 (2009).
- [13] Q. J. Wang, C. Yan, N. Yu, J. Unterhinninghofen, J. Wiersig, C. Pflügl, L. Diehl, T. Edamura, M. Yamanishi, H. Kan, and F. Capasso, *Proc. Natl. Acad. Sci. USA* **107**, 22407 (2010).
- [14] B. Redding, A. Cerjan, X. Huang, M. L. Lee, A. D. Stone, M. A. Choma, and H. Cao, *Proc. Natl. Acad. Sci. USA* **112**, 1304 (2015).
- [15] S. Sunada, T. Fukushima, S. Shinohara, T. Harayama, K. Arai, and M. Adachi, *Appl. Phys. Lett.* **104**, 241105 (2014).
- [16] H. G. L. Schwefel, N. B. Rex, H. E. Türeci, R. K. Chang, A. D. Stone, T. B. Messaoud, and J. Zyss, *J. Opt. Soc. Am. B* **21**, 923 (2004).
- [17] S. Shinohara and T. Harayama, *Phys. Rev. E* **75**, 036216 (2007).
- [18] S.-B. Lee, J. Yang, S. Moon, J.-H. Lee, K. An, J.-B. Shim, H.-W. Lee, and S.-W. Kim, *Phys. Rev. A* **75**, 011802(R) (2007).
- [19] G. Hackenbroich and J. U. Nöckel, *Europhys. Lett.* **39**, 371 (1997).
- [20] S. Shinohara, T. Harayama, T. Fukushima, M. Hentschel, T. Sasaki, and E. E. Narimanov, *Phys. Rev. Lett.* **104**, 163902 (2010); S. Shinohara, T. Harayama, T. Fukushima, M. Hentschel, S. Sunada, and E. E. Narimanov, *Phys. Rev. A* **83**, 053837 (2011).
- [21] S.-B. Lee, J.-H. Lee, J.-S. Chang, H.-J. Moon, S. W. Kim, and K. An, *Phys. Rev. Lett.* **88**, 033903 (2002).
- [22] G. D. Chern, H. E. Türeci, A. D. Stone, R. K. Chang, M. Kneissl, and N. M. Johnson, *Appl. Phys. Lett.* **83**, 1710 (2003).
- [23] M. Sargent III, M. O. Scully, and W. E. Lamb, Jr, *Laser Physics*, (Addison-Wesley Pub., Massachusetts, 1974).
- [24] M. Sargent III, *Phys. Rev. A* **48**, 717 (1993).
- [25] W. W. Chow, S. W. Koch, and M. Sargent III, *Semiconductor-Laser Physics* (Springer, 1997).
- [26] T. Harayama, P. Davis, and K. S. Ikeda, *Phys. Rev. Lett.* **90**, 063901 (2003).
- [27] S. Sunada, T. Harayama, and K. S. Ikeda, *Phys. Rev. E* **71**, 046209 (2005).
- [28] T. Harayama, S. Sunada, and K. S. Ikeda, *Phys. Rev. A* **72**, 013803 (2005).
- [29] T. Harayama, T. Fukushima, S. Sunada, and K. S. Ikeda, *Phys. Rev. Lett.* **91**, 073903 (2003).
- [30] S. Sunada, T. Fukushima, S. Shinohara, T. Harayama, and M. Adachi, *Phys. Rev. A* **88**, 013802 (2013).
- [31] H. E. Türeci, A. D. Stone, and B. Collier, *Phys. Rev. A* **74**, 043822 (2006).
- [32] L. Ge, Y. D. Chong, and A. D. Stone, *Phys. Rev. A* **82**, 063824 (2010).
- [33] L. A. Bunimovich, *Commun. Math. Phys.* **65**, 295 (1979).
- [34] M. V. Berry, *Eur. J. Phys.* **2**, 91 (1981).
- [35] T. Fukushima and T. Harayama, *IEEE J. Sel. Top. Quantum Electron.* **10**, 1039 (2004).
- [36] The contrast was defined as the standard deviation of the emission intensity distribution divided by the mean value because the intensity was distributed according to a negative exponential distribution. The definition of the contrast is similar to that reported in [14].
- [37] S. Sunada, T. Harayama, and K. S. Ikeda, *Nonlinear Phenom. Complex Syst.* **10**, 1 (2007).
- [38] M. Yamada, *IEEE J. Quantum Electron.* **19**, 1365 (1983).
- [39] J. Wiersig, *J. Opt. A: Pure and Appl. Opt.* **5**, 53 (2003).
- [40] S. Shinohara, T. Fukushima, and T. Harayama, *Phys. Rev. A* **77**, 033807 (2008).
- [41] T. Harayama, T. Fukushima, P. Davis, P. O. Vaccaro, T. Miyasaka, T. Nishimura, and T. Aida, *Phys. Rev. E* **67**, 015207(R) (2003).
- [42] W. Fang, H. Cao, and G. S. Solomon, *Appl. Phys. Lett.* **90**, 081108 (2007).
- [43] R. Audet, M. A. Belkin, J. A. Fan, B. G. Lee, K. Lin, F. Capasso, E. E. Narimanov, D. Bour, S. Corzine, J. Zhu, and G. Höfler, *Appl. Phys. Lett.* **91**, 131106 (2007).
- [44] M.-W. Kim, C.-H. Yi, S. Rim, C.-M. Kim, J.-H. Kim, and K.-R. Oh, *Opt. Express*, **20**, 13651 (2012).
- [45] M. Lebental, J. S. Laurel, R. Hierle, and J. Zyss, *Appl. Phys. Lett.* **88**, 031108 (2006).
- [46] M. Choi, S. Shinohara, and T. Harayama, *Opt. Express* **16**, 17554 (2008).